Scaling up Microbial Fuel Cells

ARTICLE *in* ENVIRONMENTAL SCIENCE AND TECHNOLOGY · NOVEMBER 2008

Impact Factor: 5.33 · DOI: 10.1021/es800775d · Source: PubMed

3 AUTHORS:

Alim Dewan
Texas A&M University
15 PUBLICATIONS **477** CITATIONS
SEE PROFILE

Haluk Beyenal
Washington State University
133 PUBLICATIONS **3,235** CITATIONS
SEE PROFILE

Zbigniew Lewandowski
Montana State University
153 PUBLICATIONS **8,104** CITATIONS
SEE PROFILE

Environ. Sci. Technol. **2008,** *42,* 7643–7648

Scaling up Microbial Fuel Cells

ALIM DEWAN,[†] HALUK BEYENAL,[†] AND ZBIGNIEW LEWANDOWSKI*[,‡]

School of Chemical Engineering and Bioengineering, Center for Environmental, Sediment, Aquatic Research, Washington State University, Pullman, Washington 99163-2710, and Center for Biofilm Engineering, Department of Civil Engineering, Montana State University, Bozeman, Montana 59717-3980

Received March 18, 2008. Revised manuscript received July 29, 2008. Accepted August 8, 2008.

The goal of this study was to quantify the relation between the surface area of the current-limiting electrode of a microbial fuel cell (MFC) and the power density generated by the MFC. *Shewanella oneidensis* (MR-1) was grown anaerobically in the anodic compartment of an MFC utilizing lactate as the electron donor. Graphite plate electrodes of various sizes were used as anodes. Commercially available air electrodes, composed of manganese-based catalyzed carbon bonded to a current-collecting screen made of platinum mesh, were used as cathodes, and dissolved oxygen was used as the cathodic reactant. The surface area of the cathode was always significantly larger than that of the anode, to ensure that the anode was the current-limiting electrode. The power density generated by the MFC decreased as the surface area of the anode increased, which fits well with the trend we detected comparing various published results. Thus, our findings bring into question the assertion that the overall power density generated by an MFC with large electrodes can be estimated by extrapolating from an electrode with a small surface area. Our results indicate that the maximum power density generated by an MFC is not directly proportional to the surface area of the anode, but is instead proportional to the logarithm of the surface area of the anode.

Introduction

Several authors have demonstrated that microbial fuel cells (MFCs) can generate energy (*1*−*8*), and it is expected that these devices can be scaled up to produce considerable amounts of energy in the future. However, the utility of MFCs is often judged based on the results of laboratory-bench-scale studies, and the question needs to be asked whether the amount of energy generated by MFCs is a linear function of their size. It appears, initially, that this should be the case: when the potential of an MFC remains constant, the current passing through the current-limiting electrode is directly proportional to the surface area of the electrode. Thus, when the surface area of the electrode increases, the power should increase proportionally. A necessary condition for this assertion to be true is that the *power density* of an MFC does not depend on the surface area of the current-limiting electrode. However, when we plotted the published results reporting power densities in various MFCs against the surface areas of their current-limiting electrodes (Figure 1), the results showed that power density decreases rapidly when the surface area of the current-limiting electrode is increased.

Figure 1 shows that the surface areas of the anodes used by various researchers (*2, 9*−*25*) dramatically affected the power density generated by the MFCs. For example, in laboratory scale-MFCs, when the projected surface area of the electrode was 2 cm^2, the reported power density amounted to an impressive 3000 mW/m (*2*) (*12, 13*), but in another work, in which the projected surface area of the anode was much larger, 232 cm^2, the reported maximum power density reached only a modest 26 mW/m^2 (*15*). The sediment microbial fuel cells which are deployed in the field also fit with the trend of decreasing power density with increasing surface area (Figure 1). For example, when the projected surface area of a sediment microbial fuel cell was 1830 cm^2, the maximum power density was 28 mW/m^2 (*2*). A similar trend is easy to detect in other published works and, as Figure 1 shows, when the surface area of the current-limiting electrode is increased dramatically, the reported power density reaches very low values. The trend shows that when the surface area is smaller than 10 cm^2, there is a steep climb in the reported power density. The decrease in power density is not profound when the surface area exceeds 50 cm^2.

Even though the trend exhibited by the data in Figure 1 is convincing, it can not be used to compute the relation between the power density and the surface area of the electrodes with confidence. The data points shown in Figure 1 were generated using different experimental systems, different electrode materials, different types of microorganisms, and different medium compositions; some of the MFCs were laboratory-scale devices operated under well-controlled conditions and some were larger-scale devices operated under field conditions—sediment MFCs oxidizing substances in benthic deposits. The results in Figure 1 raise an important question: how is power density related to the surface areas of electrodes in MFCs, specifically when defined, well-controlled experimental conditions and a single microorganism are used? The answer to this question may be the key to scaling up microbial fuel cells, and this study was designed to address this question.

The cell potentials and currents generated by MFCs are notoriously low, and the obvious approaches to scaling up these devices are analogous to manipulating a set of batteries: (1) connecting multiple MFCs in series to increase the overall potential or in parallel to increase the overall current (*26, 27*) and (2) increasing the surface area of the electrodes (*24, 28*).

The first approach—connecting several cells in series—failed with MFCs operated in open systems, i.e., in a lake, sea, or river. Increasing the potential of MFCs by connecting several cells in series works only when the devices are physically separated from each other and have their electrodes separated by cation exchange membranes. When several MFCs are placed in an open system, as in a river or an ocean, they act as membraneless devices, and connecting them in series does not increase the overall potential, as experimentally tested by our research group. Connecting MFCs without membranes in series does not work because all the electrodes are immersed in the same electrolyte and it is impossible to generate the electron cascade that is required to increase the electrical potential. In principal, increasing the cell potential of MFCs in open systems can be accomplished using external electronic circuitry, which is a complex endeavor because the commercially available electronic circuits used to increase potential require input potentials higher than those generated by MFCs.

* Corresponding author e-mail: ZL@erc.montana.edu.
[†] Washington State University.
[‡] Montana State University.

10.1021/es800775d CCC: $40.75
Published on Web 09/18/2008

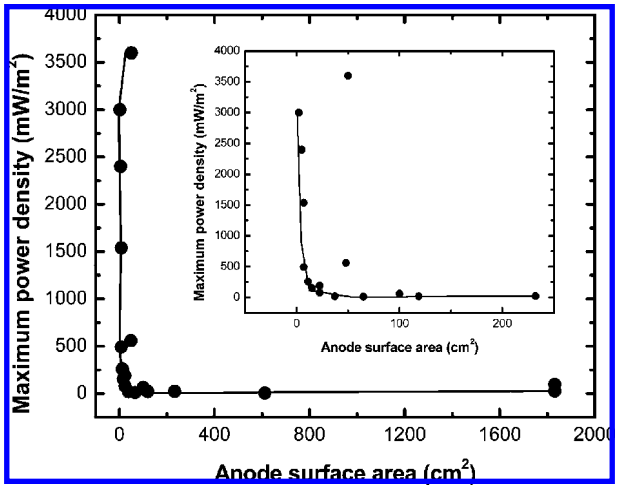

FIGURE 1. Power density vs electrode surface area. The data are from the literature (Supporting Information Table S1). The inset shows the data for smaller anode surface areas, those clumped together in the bottom left corner of the larger image.

The second approach—increasing the surface area of the electrodes—is more promising. If the MFC potential remains constant, the current—and thus the power—is directly proportional to the surface area of the electrode. This is true only if the size of the electrode surface does not affect the power density, which is not the case, as shown in Figure 1. This deviation from expectations can be related to factors that are well-known but that may not be easy to quantify in specific situations. For example, it is known that the relation between the surface area of the electrode and the power density of the MFC is affected by the mechanism (direct or mediated) of mass transport to the electrode, and it is expected that it is also affected by the mechanism of electron transport across the biofilm layer deposited on the electrode surface. The goal of this study was to quantify the relation between the surface area of an anode and the power density of the MFC. We used a two-compartment microbial fuel cell and equipped the anodic compartment with electrodes of various surface areas. Thus, we could vary the surface area of the anode and monitor the resulting changes in power density. *Shewanella oneidensis* (MR-1) were grown in the anodic compartment, using lactate as the electron donor. Under anaerobic conditions *Shewanella oneidensis* (MR-1) oxidize lactate to acetate by using the anode as electron acceptor (*29*). In our experimental system, all electrodes were immersed in the same solution, and all biofilms were exposed to the same lactate concentration and subjected to the same hydrodynamic conditions, to satisfy the conditions that were critical to our experimental design. In the cathodic compartment, dissolved oxygen was reduced on an air electrode. Voltammetric and amperometric tests were used to characterize the power output of the MFC, whereas anodes with various surface areas were used. To quantify the effect of biofilm on the relation between the surface area of the anode and the power density generated by the MFC, we evaluated the same relation in an abiotic system—without the biofilm—using the same configuration as that in the fuel cell except for the reactants: ferricyanide was used as the cathodic reactant and 2-hydroxy-1,4-naphthoquinone as the anodic reactant. Comparing the results obtained in cells with and without microorganisms elucidated the role of the biofilm on the relation between the surface area of the anode and the power density.

Materials and Methods

Microbial Fuel Cell. We used the microbial fuel cell shown in Supporting Information Figure S1. It consisted of two compartments made of polycarbonate, 800 mL liquid volume each, separated by a cation exchange membrane ESC-7000 (Electrolytica Corporation, 770-410-9166) which was sealed with rubber gaskets on both sides to prevent liquid from leaking from one compartment to the other. The electrodes were placed against the cation exchange membrane, parallel to the cathode (Supporting Information Figure S1), so that the distance between the anode and the cathode was about 1 mm. The compartments were covered with polycarbonate plates furnished with openings to make electrical connections with the electrodes. The cover plates and the compartments were sealed using gaskets to prevent leakage, and long screws with wing nuts were used to hold the reactor together. We used silicone rubber tubes to deliver liquids and gases and to remove them from the respective compartments. To prevent contamination, all outlets were equipped with flow breakers.

The anodes were made of graphite plates (Graphite-Store.com, Inc.) We used a total of seven anodic electrodes, with projected surface areas of 1.92, 4.26, 12.8, 38.8, 63.4, 92, and 155 cm^2, respectively.

The cathode was an air electrode (two pieces, each 23 cm $\times$ 9 cm) composed of manganese-based catalyzed carbon bonded to a current-collecting screen made of platinum mesh (Electric Fuel Limited). Even though this is an air electrode, we used it as a submersed electrode because the catalytic properties of the surface enhanced dissolved oxygen reduction. It had a projected surface area of 828 cm^2, which exceeded the surface area of each of the anodes specified above; to ensure that the anode was the current-limiting electrode, the surface area of the cathode was always at least 5 times larger than the surface area of the anode. The cathode potential remained constant in all experiments, demonstrating that this electrode was not limiting the current. Insulated copper wires were used to connect the electrodes to the external circuit. The copper wires were tied with the platinum wire of the mesh and then the connections were covered with silicon rubber so that electrolyte could not reach the copper wire; the electrical resistances of the connections were less than 1 Ω.

To prevent swelling, cation exchange membranes were preconditioned before the MFC was assembled by being rinsed with water and kept in a 1 M NaCl solution for 24 h. Since we reused the membranes, after each run the membrane was removed from the cell, rinsed gently with tap water to remove the deposit from the surface, kept in 80 °C water for 1 h, rinsed again and inspected visually to make sure there was no deposit on the surface. Cleaned membranes were kept in a solution of 1 M NaCl.

Microorganism, Growth Medium, Buffer and Electrolyte Solution. In the anodic compartment, *Shewanella oneidensis* (MR-1) was grown anaerobically. We used different growth mediums for inoculation and electricity production. The growth medium used for inoculation was Luria−Bertani (LB) broth, a solution of 10 g/L tryptone, 5 g/L NaCl, and 5 g/L yeast extract. During inoculation using LB medium, air was pumped to the anodic compartment for 24 h. Then we replaced the air with nitrogen and fed the reactor with the growth medium for electricity generation. The composition of the medium used for electricity generation in the MFC (*30*) was 0.1 g/L PIPES buffer, 0.78 g/L KH_2PO_4, 0.47 g/L Na_2HPO_4, 1.5 g/L NH_4Cl, 0.1 g/L KCl, 1.75 g/L NaCl, 11.23 g/L Na-Lactate, 10 mL/L mineral solution (100×), 1 g/L yeast extract, 0.05 g/L ferric NTA solution, and 10 mL/L amino acid solution (100×). The composition of the mineral solution was 1.5 g/L $C_6H_9NO_3$ (nitrilo triacetic acid), 3 g/L $MgSO_4 \cdot 7H_2O$, 0.5 g/L $MnSO_4 \cdot H_2O$, 1 g/L NaCl, 0.1 g/L $FeSO_4 \cdot 7H_2O$, 0.1 g/L $CaCl_2 \cdot 2H_2O$, 0.1 g/L $CoCl_2 \cdot 6H_2O$, 0.13 g/L $ZnCl_2$, 0.01 g/L $CuSO_4 \cdot 5H_2O$, 0.01 g/L $AlK(SO_4)_2 \cdot 12H_2O$, 0.01 g/L H_3BO_3, 0.025 g/L $Na_2MoO_4 \cdot 2H_2O$, 0.025 g/L $NiCl_2 \cdot 6H_2O$ and 0.025

g/L $Na_2WO_4 \cdot 2H_2O$. The composition of the amino acid solution was 2 g/L L-glutamic acid, 2 g/L L-arginine and 2 g/L DL-serine. The ferric NTA stock was made of 16.4 g/L $NaHCO_3$ and 27 g/L $FeCl_3 \cdot 6H_2O$. The mineral, amino acid, and ferric NTA solution was filtered and stored in a fridge. The pH of the growth medium was adjusted to 7 using NaOH or HCl solution.

The solution in the cathodic compartment was a phosphate buffer (pH 7): 1.825 g/L Na_2HPO_4, 0.35 g/L KH_2PO_4, adjusted to pH 7.0 using 0.1 M HCl.

MFC Startup and Operation. The startup operation involved several steps, which can be summarized as follows: 1. clean the MFC parts and prepare the membrane, 2. assemble the MFC, 3. connect the silicon tubing and flow breakers, fill the compartments with deionized water and close the ports using stoppers; 4. autoclave the fuel cell at 121 °C for 30 min, 5. replace the deionized water with buffer in the cathodic compartment and with growth medium in the anodic compartment, 6. insert the Ag/AgCl reference electrode into the cathodic compartment, 7. inoculate the MFC with *Shewanella oneidensis* (MR-1), 8. replace 100 mL of buffer from the cathodic compartment daily, 9. pump air continuously to the cathodic compartment and 10. pump N_2 continuously to the anodic compartment.

Initially, the reactor was operated in batch mode for one day, after which the growth medium was pumped continuously to the anodic compartment at 8.33 mL/h using a peristaltic pump. Air was pumped to the cathodic compartment continuously and at a constant rate.

For the first few days, the MFC was operated without an electrical load. After the open circuit potential reached 0.76 V, the electrodes were connected through a resistor, 1000Ω, as shown in Supporting Information Figure S1. The MFC was operated for 5 months continuously, and the measurements described in the following sections were performed with the electrodes connected through the resistor or disconnected when individual electrodes were polarized using a potentiostat. When the electrodes were polarized using the potentiostat, we disconnected the resistor from the MFC and waited until the electrodes reached the open circuit potential before applying polarization potential.

Measurements and Calculations. *Potentiodynamic Polarization.* We used a potentiostat (Reference 600, Gamry Instruments, Inc.) and a three-electrode system with the anode as the working electrode, the cathode as the auxiliary electrode and Ag/AgCl as the reference electrode. The anode potentials were scanned from a potential 0.1 V lower than the open circuit potential of the anode to 0.05 V higher than the open circuit potential of the cathode—both measured against the Ag/AgCl reference electrode—using a step size of 0.01 V and a sampling time of 0.1 s (scan rate 0.1 V/sec). The potential of the anode and the current between the anode and the cathode were monitored using the potentiostat, while the cathode potential was monitored using a HP data logger (HP model no. 34970A) to verify that the cathode was not the current-limiting electrode. Potentiodynamic polarization in absence of biofilms using abiotic system of ferricyanide as the cathodic reactant and 2-hydroxy-1,4-naphthoquinone as the anodic reactant are described in the Supporting Information.

The cell potential was calculated as the difference between the potentials of the anode and the cathode. The power is calculated as the product of the cell potential and the current flowing between the electrodes (power = cell potential × current). Power density is evaluated by dividing the overall power generated by the surface area of the current-limiting electrode.

Impedance Spectroscopy. It is known that the internal resistance of an MFC affects the power generated by the cell (*21, 31*). We consider the internal resistance of an MFC to be the sum of the following electrical resistances: the electrical resistance of the electrolyte, the equivalent electrical resistance reflecting the mass transport limitation (diffusion resistance) and the equivalent electrical resistance reflecting the activation energy barrier of the redox reaction occurring at the electrode surface (charge transfer resistance). To ensure that the electrical resistance of the electrolyte remained constant, the electrolyte always had the same composition and the distances between the electrodes were always the same. To quantify the equivalent electrical resistances reflecting the mass transport limitation and the activation energy barrier, we used electrochemical impedance spectroscopy (EIS) on two electrodes. EIS measurements were performed in MFCs with anodes covered with biofilm. For control experiments using soluble electron shuttles, there was no biofilm on the electrodes. In all measurements, the anodes were used as the working electrodes and the cathodes as the counter electrodes. The impedance spectra were measured with a Gamry potentiostat (Reference 600, Gamry Instruments, Inc.) using the frequency range between 10^5 and 1 Hz and a sinusoidal perturbation with a 10 mV amplitude. From the impedance data, Nyquist plots were drawn showing the real part of the impedance on the *x*-axis and the imaginary part on the *y*-axis. The Nyquist plot consists of a semicircle and a linear portion. The semicircle portion represents the charge transfer resistance and the linear portion represents the diffusion resistance (R_t). $R_{\Omega,}$ represents the resistance of the electrolyte. The internal resistance (R_Ω + Rt) was calculated from the Nyquist plot as described by He et al. (*32*). The distance between the zero and the first intersection of the semicircle with the *x*-axis of the Nyquist plot, where the imaginary part of the impedance is zero, is the electrolyte resistance. The distance between the first intersection and the second intersection is the sum of the charge transfer and the diffusion resistances (R_t).

Results and Discussion

The polarization experiments were run repeatedly during the 5 months of operation of the MFC and we consistently observed similar results. In repeated experiments we had identical behaviors. Here we report only results that are representative of several measurements taken under the same conditions.

Figure 2A plots cell potential vs power density for electrodes (anodes) with various surface areas. From these data, we estimated the maximum power density for each setup, and maximum power density is plotted against anode surface area in Figure 2B. The potentiodynamic polarization experimental results show the maximum power density was delivered by the electrode with the smallest surface area (1.92 cm^2, Figure 2B) and that the power density decreased when the surface area of the electrode was increased (Figure 2B). The maximum power density was 0.329 mW/cm^2, for the smallest electrode (1.92 cm^2). Increasing the surface area 80 times (to 155 cm^2) lowered the power density to less than half of that measured for the electrode with the smallest surface area (0.141 mW/cm^2).

The data in Figure 2B resemble those plotted in Figure 1. The power density is not linearly correlated with electrode surface area: it decreases with increasing electrode surface area. The decrease in measured power may be explained, to some extent at least, by the edge effect of the smaller electrodes and the fact that the mass transport of electroactive species to microelectrodes is spherical rather than linear: it is well-known that very small electrodes, such as microelectrodes, deliver higher current densities than large electrodes (*33*). However, all our electrodes were significantly larger than those typically considered to be microelectrodes, which demonstrates that there must have been another factor, besides the edge effect and mass transport, involved

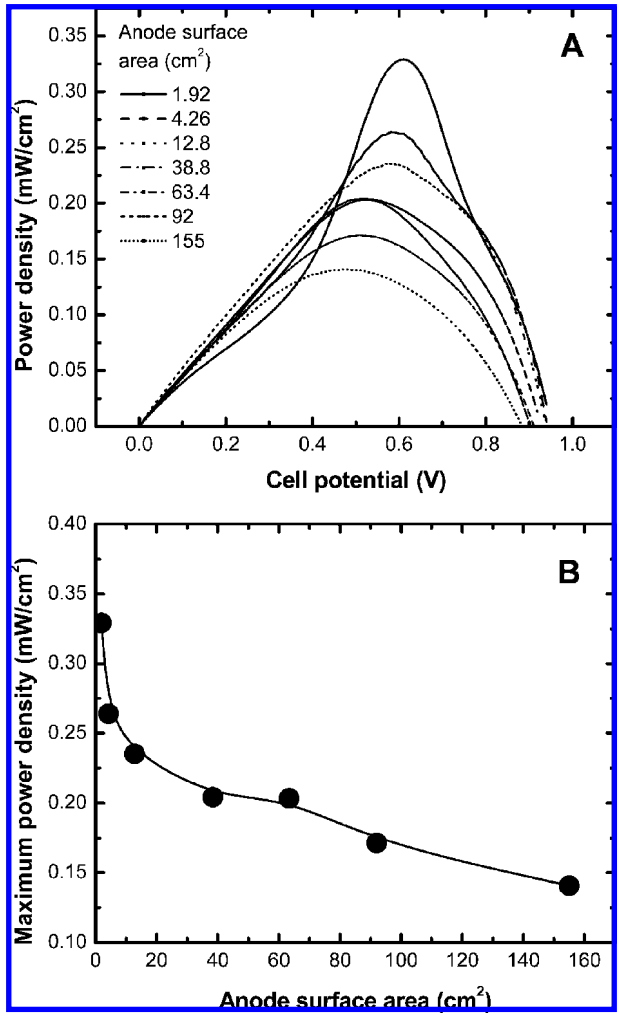

FIGURE 2. (A) Characterization of MFC electrodes using voltammetry. All anodes were scanned from −0.8$V_{Ag/AgCl}$ to 0. Two $V_{Ag/AgCl}$ using a potential step size of 0.01 V, and the sampling time for each step was 0.1 s (scan rate 0.1 V/sec). (B) The maximum power densities, calculated from the results in Figure A, are plotted against the surface areas of the electrodes.

in the observed relations. It is worth noting that the literature data quantifying the edge effect and current densities in microelectrodes were all acquired using electrodes without surface deposits. Therefore, we hypothesize that the effect of surface biofilm deposits on the electron transfer rate may have been the reason for the observed difference between the power densities delivered by small and large electrodes. However, this effect has not been quantified adequately, and this explanation remains hypothetical.

Figure 1 compiles results that were published by many authors using a variety of experimental systems and experimental conditions. Our results, shown in Figure 2A, qualitatively fit those shown in Figure 1.

Polarization Curves in the Presence and Absence of Biofilm. As explained in the Materials and Methods, potentiodynamic polarization tests were conducted using two systems: one with the anodes covered with biofilm and one without biofilm.

Supporting Information Figure S2 shows characteristic potentiodynamic curves, acquired in the abiotic solution. All curves show the peak at the same potential, −0.08 $V_{Ag/AgCl}$. The potentiodynamic curves collected in the presence of biofilm on the electrode surface, Figure 3, are more complex. For the two smallest electrodes we see a current peak at potential −0.38 $V_{Ag/AgCl}$ which is not present in the

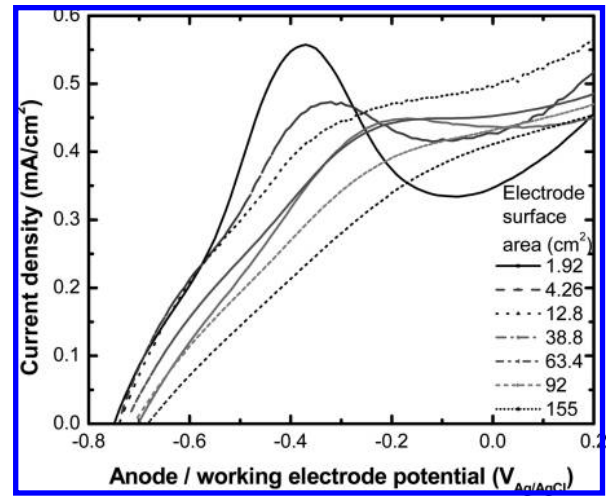

FIGURE 3. Electrode potential in the presence of biofilm vs current density. The electrodes were scanned from −0.8 $V_{Ag/AgCl}$ to 0.2 $V_{Ag/AgCl}$ at a step size of 0.01 V, and the sampling time was 0.1 s for each step (scan rate 0.1 V/sec, pH 7.0).

polarization curves for the electrodes with larger surface areas. Figure 3 also shows that the maximum current density corresponding to the potential of a biofilm-covered electrode varied with the size of the electrode: when a 1.92-cm² anode was used, the maximum current density was at −0.38 $V_{Ag/AgCl}$, but when a 155 cm² anode was used, the maximum current density was at 0.2 $V_{Ag/AgCl}$. Since the peak current density for soluble chemicals is at the same potential, independently of the size of the electrode (like the data in Supporting Information Figure S2), the presence of the biofilm must affect the mechanism and the rate of electron transfer to the electrode. This effect seems to be more pronounced when the surface of the electrode is small. It is also possible that the presence of the biofilm and the growth medium introduced many redox-sensitive species that could discharge at various potentials, an effect that was nonexistent when the electrolyte was a solution of a well-defined electroactive substance in the absence of biofilm. It is possible that the mechanism of electron transfer from the dissolved substances in solution to the solid electrodes, via the biofilm, plays a critical role in establishing the relation between the surface area of the electrodes and the power density generated by the MFC.

Internal Resistance of the MFC. It is possible that the power density decreased because of the increased internal resistance of the cell. This assertion, however, is not supported by the results shown in Supporting Information Figure S3, in which internal resistance decreased with increasing surface area of the anode. We therefore conclude that the observed decrease in power density was not caused by the increase in the internal resistance of the cell. The internal resistance of the electrodes used in the control experiments had a similar trend. In the control experiment, for the electrodes with surface areas of 4.26, 12.8, 23.6, and 39.6 cm², the internal resistances were 6.9, 3.8, 3.6, and 2.5 Ω, respectively. The power densities decreased despite the internal resistance decreasing, because the electron transfer was limited not by the internal resistance but by the rate of the electrode reaction or by the rate of the microbial reaction.

Power Density at a Constant Cell Potential. To measure the power density at a constant cell potential, the anodes of the MFC were polarized to a constant potential using the potentiostat, and the results are shown in Figure 4. As expected, at a constant cell potential, the power density shows the same trend: it decreases as the surface area of the electrode increases (Figure 4). Keeping the anode potential constant using a potentiostat ensured that the anode was not the

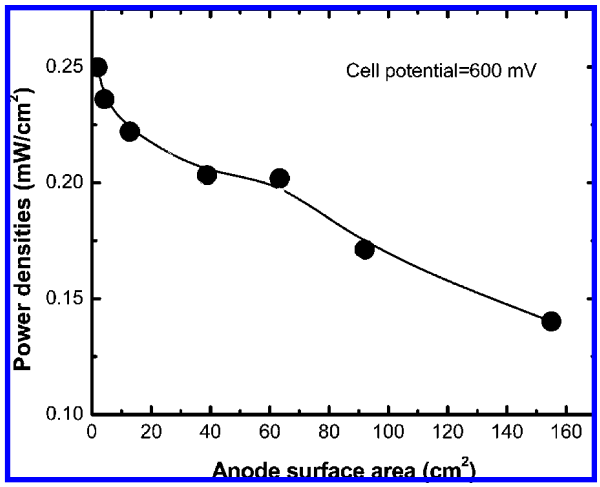

FIGURE 4. Variation of power density with electrode surface area at a constant cell potential.

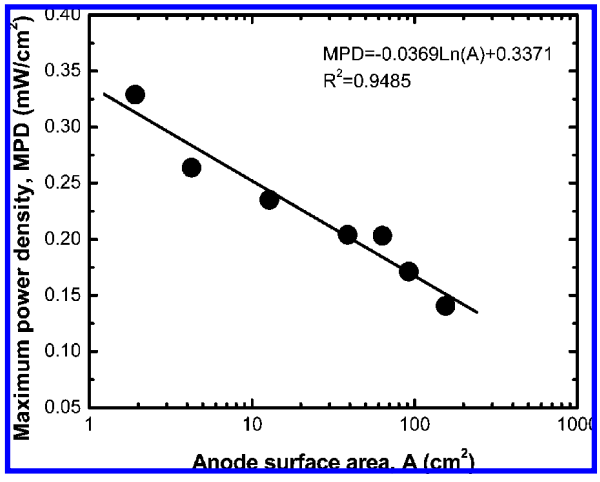

FIGURE 5. Ln (surface area) and power density correlate linearly.

current-limiting electrode. In repeated experiments we consistently observed the same trend. We speculate that this is because, in biofilms, various redox reactions are activated at different potentials.

Practical Significance. The main conclusions of our study are that in MFCs power density decreases with increasing surface area of the current-limiting electrode and that when scaling up microbial fuel cells, one cannot assume that power density will remain constant with the increased electrode surface area. The actual surface area required to generate the desired power will have to be much higher than that predicted from a linear relationship and the results of measurements using small electrode surface areas. From our measurements, the relation between the surface area and the power density can be linearized on a logarithmic scale as shown in Figure 5:

$$\text{maximum power density} = -0.0369 \times \ln(\text{surface area}) + 0.3371 \quad (1)$$

To produce the relation between the surface area of the anode and the maximum power density we used all the experimental data produced in this work. Equation 1 gives a good regression coefficient ($R^2 = 0.95$). It is important to note that even though the trend exhibited by our data is the same as that shown in Figure 1, the data in Figure 1 do not fit this logarithmic relationship. This may be due to a variety of causes but the different experimental conditions used to generate the data points in Figure 1 discourage mechanistic interpretations of the observed differences. Our data were generated in a consistent way in a well-controlled system, while Figure 1 is a compilation of many results obtained in many systems. Our overall conclusion is consistent with that seen in the data compiled in Figure 1: in MFCs, power density is a nonlinear function of the surface area of the current-limiting electrode.

Acknowledgments

We gratefully acknowledge the financial support provided by grant no. N00014-06-1-0217 from the U.S. Office of Naval Research (ONR).

Supporting Information Available

Three additional figures and one table. This material is available free of charge via the Internet at http://pubs.acs.org.

Literature Cited

(1) Allen, R. M.; Bennetto, H. P. Microbial fuel cells—Electricity production from carbohydrates. *Appl. Biochem. Biotechnol.* **1993**, *39*, 27–40.
(2) Tender, L. M.; Reimers, C. E.; Stecher, H. A.; Holmes, D. E.; Bond, D. R.; Lowy, D. A.; Pilobello, K.; Fertig, S. J.; Lovley, D. R. Harnessing microbially generated power on the seafloor. *Nat. Biotechnol.* **2002**, *20*, 821–825.
(3) Aelterman, P.; Rabaey, K.; Clauwaert, P.; Verstraete, W. Microbial fuel cells for wastewater treatment. *Water Sci. Technol.* **2006**, *54*, 9–15.
(4) Rhoads, A.; Beyenal, H.; Lewandowski, Z. Microbial fuel cell using anaerobic respiration as an anodic reaction and biomineralized manganese as a cathodic reactant. *Environ. Sci. Technol.* **2005**, *39*, 4666–4671.
(5) Logan, B. E.; Regan, J. M. Microbial challenges and applications. *Environ. Sci. Technol.* **2006**, *40*, 5172–5180.
(6) Lovley, D. R. Bug juice: Harvesting electricity with microorganisms. *Nat. Rev. Microbiol.* **2006**, *4*, 497–508.
(7) Pham, T. H.; Rabaey, K.; Aelterman, P.; Clauwaert, P.; De Schamphelaire, L.; Boon, N.; Verstraete, W. Microbial fuel cells in relation to conventional anaerobic digestion technology. *Eng. Life Sci.* **2006**, *6*, 285–292.
(8) Reimers, C. E.; Girguis, P.; Stecher, H. A., III; Tender, L. M.; Ryckelynck, N. Microbial fuel cell energy from an ocean cold seep. *Geobiology* **2006**, *4*, 123–136.
(9) Min, B. K.; Cheng, S. A.; Logan, B. E. Electricity generation using membrane and salt bridge microbial fuel cells. *Water Res.* **2005**, *39*, 1675–1686.
(10) Ren, Z.; Ward, T. E.; Regan, J. M. Electricity Production from Cellulose in a Microbial Fuel Cell Using a Defined Binary Culture. *Environ. Sci. Technol.* **2007**, *41*, 4781–4786.
(11) Lowy, D. A.; Tender, L. M.; Zeikus, J. G.; Park, D. H.; Lovley, D. R. Harvesting energy from the marine sediment-water interface II - Kinetic activity of anode materials. *Biosens. Bioelectron.* **2006**, *21*, 2058–2063.
(12) Ringeisen, B. R.; Henderson, E.; Wu, P. K.; Pietron, J.; Ray, R.; Little, B.; Biffinger, J. C.; Jones-Meehan, J. M. High power density from a miniature microbial fuel cell using Shewanella oneidensis DSP10. *Environ. Sci. Technol.* **2006**, *40*, 2629–2634.
(13) Ringeisen, B. R.; Ray, R.; Little, B. A miniature microbial fuel cell operating with an aerobic anode chamber. *J. Power Sources* **2007**, *165*, 591–597.
(14) Liu, Z. D.; Li, H. R. Effects of bio- and abio-factors on electricity production in a mediatorless microbial fuel cell. *Biochem. Eng. J.* **2007**, *36*, 209–214.
(15) Liu, H.; Ramnarayanan, R.; Logan, B. E. Production of electricity during wastewater treatment using a single chamber microbial fuel cell. *Environ. Sci. Technol.* **2004**, *38*, 2281–2285.
(16) Min, B.; Logan, B. E. Continuous electricity generation from domestic wastewater and organic substrates in a flat plate microbial fuel cell. *Environ. Sci. Technol.* **2004**, *38*, 5809–5814.
(17) Tartakovsky, B.; Guiot, S. R. A comparison of air and hydrogen peroxide oxygenated microbial fuel cell reactors. *Biotechnol. Prog.* **2006**, *22*, 241–246.
(18) Oh, S. E.; Logan, B. E. Proton exchange membrane and electrode surface areas as factors that affect power generation in microbial fuel cells. *Appl. Microbiol. Biotechnol.* **2006**, *70*, 162–169.
(19) Liu, H.; Logan, B. E. Electricity generation using an air-cathode single chamber microbial fuel cell in the presence and absence of a proton exchange membrane. *Environ. Sci. Technol.* **2004**, *38*, 4040–4046.

(20) Oh, S.; Min, B.; Logan, B. E. Cathode performance as a factor in electricity generation in microbial fuel cells. *Environ. Sci. Technol.* **2004**, *38*, 4900–4904.

(21) Cheng, S.; Liu, H.; Logan, B. E. Increased power generation in a continuous flow MFC with advective flow through the porous anode and reduced electrode spacing. *Environ. Sci. Technol.* **2006**, *40*, 2426–2432.

(22) Moon, H.; Chang, I. S.; Kim, B. H. Continuous electricity production from artificial wastewater using a mediator-less microbial fuel cell. *Bioresour. Technol.* **2006**, *97*, 621–627.

(23) Rabaey, K.; Lissens, G.; Siciliano, S. D.; Verstraete, W. A microbial fuel cell capable of converting glucose to electricity at high rate and efficiency. *Biotechnol. Lett.* **2003**, *25*, 1531–1535.

(24) Logan, B.; Cheng, S.; Watson, V.; Estadt, G. Graphite fiber brush anodes for increased power production in air-cathode microbial fuel cells. *Environ. Sci. Technol.* **2007**, *41*, 3341–3346.

(25) Min, B.; Kim, J.; Oh, S.; Regan, J. M.; Logan, B. E. Electricity generation from swine wastewater using microbial fuel cells. *Water Res.* **2005**, *39*, 4961–4968.

(26) Aelterman, P.; Rabaey, K.; Pham, H. T.; Boon, N.; Verstraete, W. Continuous electricity generation at high voltages and currents using stacked microbial fuel cells. *Environ. Sci. Technol.* **2006**, *40*, 3388–3394.

(27) Shin, S. H.; Choi, Y. J.; Na, S. H.; Jung, S. H.; Kim, S. Development of bipolar plate stack type microbial fuel cells. *Bull. Korean Chem. Soc.* **2006**, *27*, 281–285.

(28) Kim, H. J.; Park, H. S.; Hyun, M. S.; Chang, I. S.; Kim, M.; Kim, B. H. A mediator-less microbial fuel cell using a metal reducing bacterium, Shewanella putrefaciense. *Enzyme Microb. Technol.* **2002**, *30*, 145–152.

(29) Lanthier, M.; Gregory, K. B.; Lovley, D. R. Growth with high planktonic biomass in *Shewanella oneidensis* fuel cells. *FEMS Microbiol. Lett.* **2008**, *278*, 29–35.

(30) Gorby, Y. A.; Yanina, S.; Mclean, J. S.; Rosso, K. M.; Moyles, D.; Dohnalkova, A.; Beveridge, T. J.; Chang, I. S.; Kim, B. H.; Kim, K. S.; Culley, D. E.; Reed, S. B.; Romine, M. F.; Saffarini, D. A.; Hill, E. A.; Shi, L.; Elias, D. A.; Kennedy, D. W.; Pinchuk, G.; Watanabe, K.; Ishii, S.; Logan, B.; Nealson, K. H.; Fredrickson, J. K. Electrically conductive bacterial nanowires produced by Shewanella oneidensis strain MR-1 and other microorganisms. *Proc. Natl. Acad. Sci. U. S. A.* **2006**, *103*, 11358–11363.

(31) Menicucci, J.; Beyenal, H.; Marsili, E.; Veluchamy, R. A.; Demir, G.; Lewandowski, Z. Procedure for determining maximum sustainable power generated by microbial fuel cells. *Environ. Sci. Technol.* **2006**, *40*, 1062–1068.

(32) He, Z.; Wagner, N.; Minteer, S. D.; Angenent, L. T. An upflow microbial fuel cell with an interior cathode: assessment of the internal resistance by impedance spectroscopy. *Environ. Sci. Technol.* **2006**, *40*, 5212–5217.

(33) Bard, A. J., and Faulkner, L. R. *Electrochemical methods: Fundamentals and applications, 2*; John Wiley & Sons, Inc.: New York, 2001; pp 155−221.

ES800775D